Heterochromatin and *tri*-methylated lysine 20 of histone H4 in animals

Niki Kourmouli[1], Peter Jeppesen[1], Shantha Mahadevhaiah[2], Paul Burgoyne[2], Rong Wu[3], David M. Gilbert[3], Silvia Bongiorni[4], Giorgio Prantera[4], Laura Fanti[5], Sergio Pimpinelli[5], Wei Shi[6], Reinald Fundele[6] and Prim B. Singh[1,*]

[1]Nuclear Reprogramming Laboratory, Division of Gene Expression and Development, Roslin Institute, Edinburgh, EH25 9PS, UK
[2]Laboratory of Developmental Genetics, National Institute for Medical Research, Mill Hill, London, NW7 1AA, UK
[3]Department of Biochemistry and Molecular Biology, SUNY Upstate Medical University, 750 East Adams Street, Syracuse, NY 13210, USA
[4]Dipartimento di Agrobiologia e Agrochimica, Università della Tuscia, Via San C. De Lellis, Viterbo, 01100, Italy
[5]Dipartimento di Genetica e Biologia molecolare, Università di Roma 'La Sapienza', Piazzale Aldo Moro, Roma, 00185, Italy
[6]Uppsala University, Department of Development and Genetics, Norbyvagen 18A, Uppsala, 75236, Sweden
*Author for correspondence (e-mail: prim.singh@bbsrc.ac.uk)

Accepted 25 March 2004
Journal of Cell Science 117, 2491-2501 Published by The Company of Biologists 2004
doi:10.1242/jcs.01238

Summary

Tri-methylated lysine 20 on histone H4 (Me(3)K20H4) is a marker of constitutive heterochromatin in murine interphase and metaphase cells. Heterochromatin marked by Me(3)K20H4 replicates late during S phase of the cell cycle. Serum starvation increases the number of cells that exhibit high levels of Me(3)K20H4 at constitutive heterochromatin. Me(3)K20H4 is also present at the centromeric heterochromatin of most meiotic chromosomes during spermatogenesis and at the pseudoautosomal region, as well as at some telomeres. It is not present on the XY-body. During murine embryogenesis the maternal pronucleus contains Me(3)K20H4; Me(3)K20H4 is absent from the paternal pronucleus. On *Drosophila* polytene chromosomes Me(3)K20H4 is present in a 'punctate pattern' at many chromosomal bands, including the chromocenter. In coccids it is present on the facultatively heterochromatinised paternal chromosome set. We also present evidence that Me(3)K20H4 is dependent upon H3-specific Suv(3)9 histone methyltransferase activity, suggesting that there may be 'epigenetic cross-talk' between histones H3 and H4.

Key words: Heterochromatin, Epigenetics, Histone code

Introduction

Heterochromatin comes in two major types – constitutive and facultative (Brown, 1966). Constitutive heterochromatin is typically found at specific chromosomal domains including the centromeres, telomeres and nucleolar organiser regions (Heitz, 1928; McClintock, 1934). It also replicates late in S-phase (Lima-de-Faria and Jaworska, 1968), is enriched in repetitive sequences (John and Miklos, 1979) and is relatively depleted in the number of genes it contains (Pimpinelli et al., 1986). The molecular characterisation of constitutive heterochromatin has revealed that the DNA is highly methylated (Miller et al., 1974) and that its constituent histones are enriched in methylated lysine 9 of histone H3 [MeK9H3 (Peters et al., 2001; Cowell et al., 2002)], yet depleted in both methylated lysine 4 of histone H3 (MeK4H3 [(Boggs et al., 2002)] and acetylated histone H4 [AcH4 (Jeppesen et al., 1992)]. The MeK9H3 found at sites of peri-centromeric heterochromatin in mouse cells results from the enzymatic activity of H3-specific histone methyltransferases, called Suv(3)9h1 and h2 (Rea et al., 2000), and their activity forms a 'platform' of MeK9H3 for the recruitment of heterochromatin protein 1 [HP1 (Bannister et al., 2001; Jacobs et al., 2001; Lachner et al., 2001)].

Unlike constitutive heterochromatin, facultative heterochromatin is developmentally regulated and was defined on the basis of early work in *Sciara* and coccids (Brown, 1966). In the coccid system the paternal set of chromosomes is facultatively heterochromatinised during development in males (Brown and Nur, 1964). In female mammals there is a similar facultative heterochromatinisation that occurs during development, giving rise to an inactive X chromosome [X_i (Lyon, 1999)]. X-inactivation in female mammals has certain similarities to constitutive heterochromatin: the X_i is replicated late in S-phase (Morishima et al., 1962), retains a condensed heterochromatic morphology during interphase, called the Barr body (Barr and Bertram, 1949), and is depleted in both MeK4H3 and AcH4 (Boggs et al., 2002). Immunoprecipitation and immunofluorescence experiments have shown that the X_i is enriched in MeK9H3 and methylated K27 on H3 (MeK27H3) (Peters et al., 2002; Boggs et al., 2002; Cowell et al., 2002; Plath et al., 2003). In human interphase nuclei, HP1 localises to the X_i (Chadwick and Willard, 2003).

Recent studies on methylated histones have revealed that the level of methylation of the specific lysines may have important functional consequences for the assembly of (hetero)chromatin domains. Each lysine residue can accept up to three methyl groups forming mono-, di- and tri-methylated derivatives with the increase in methylation state resulting in a concomitant increase in hydrophobicity of the histone tail. Active genes appear to be *tri*-methylated at lysine 4 on histone H3 (Santos-Rosa et al., 2002) in *Saccharomyces cerevisiae* and, in *Neursopora crassa*, *tri*-methylation of lysine 9 on histone H3 is a prerequisite for DNA methylation and the

assembly of a repressed, heterochromatic state (Tamaru et al., 2003).

On the N-terminal tail of histone H4 the lysine residue that is methylated is lysine 20. The dimethylated form of K20H4 (Me(2)K20H4) has been investigated in some detail and shown to be associated with euchromatin in mammalian cells (Rice et al., 2002; Nishioka et al., 2002; Fang et al., 2002). Because of the evidence that the degree of methylation might have important functional consequences for (hetero)chromatin assembly we decided to make an antibody that specifically recognises *tri*-methylated lysine 20 of histone H4 (Me(3)K20H4). Using this specific reagent we have shown that Me(3)K20H4 localises to heterochromatin, unlike Me(2)K20H4, and that Me(3)K20H4 is tightly linked to the presence of Me(3)K9H3, suggesting that there is epigenetic cross-talk between histones H3 and H4.

Materials and Methods

Antibody production and characterisation

We synthesised the peptide GGAKRHR**K**VLRDNIQC, corresponding to amino-acids 13-27 of histone H4, where the underlined **K** was trimethylated (Bachem). The peptide was rendered immunogenic by coupling to the carrier protein tuberculin PPD (De Silva et al., 1999) using sulfo-SMCC (Pierce Chemical Company). A cysteine residue was added to the carboxyl end of the peptide during synthesis to facilitate conjugation. Two BCG-vaccinated rabbits were injected with the conjugate every 2 weeks and bleeds taken for testing by ELISA. Screening the sera on *tri*-methyl K20H4 peptide and the unmodified peptide revealed that rabbit 2 had generated a specific, high-titre, response to the *tri*-methyl K20H4 peptide (data not shown). Sera from this animal were used for all experiments. Before use, the serum from this animal was twice passed over an agarose (Severnlink Iodoacetyl Agarose) column to which the unmodified peptide was coupled in order to remove any residual activity.

For immunoblotting, histones from different sources were analysed in a 13.5% SDS-polyacrylamide gel, transferred to nitrocellulose and blotted as described previously (Maison et al., 1993; Maison et al., 1995). Twelve μg of calf thymus histones (Roche), 12 μg of turkey erythrocyte histones isolated by hydroxyapatite chromatography, 3 μg of recombinant H4 (Upstate) and 50 μg of turkey erythrocyte nuclei were used. The anti-Me(3)K20H4 anti-serum was used at a dilution 1:500 and binding was detected using a donkey anti-rabbit HRP-conjugated secondary antibody (Amersham) at a dilution 1:10,000.

To test the specificity of the antiserum in western blotting and competition assays we synthesised the corresponding mono- and di-methylated K20H4 peptides. Two-fold serial dilutions of these peptides as well as the unmodified and trimethylated peptides were spotted on nitrocellulose (spotted quantities from 1.6 mg to 50 ng) and blotted with the antiserum. For competition experiments the antiserum was pre-incubated with 0.1 μg/ml of each peptide prior to western blotting.

The specificity of the staining was also tested by immunofluorescence. The anti-Me(3)K20H4 serum was diluted 1:100 and pre-incubated with 1.5-3 ng/ml of the unmodified, mono-, di- and tri-metylated peptides, as well as a peptide of H3 trimethylated at lysine 9, before staining C127 cells as described below.

Immunofluorescence detection of Me(3)K20H4 in mouse interphase nuclei

Indirect immunofluorescence with C127, wild-type and double null *Suv39h1* and *Suv39h2* double-null mouse embryonic fibroblasts (a gift from T. Jenuwein) was performed as described previously (Maison et al., 1993; Maison et al., 1995). The anti-Me(3)K20H4 serum was used at a dilution 1:100 and detected by an Alexa fluor 488 goat anti-rabbit IgG. The specimens were viewed with a Zeiss Axiovert S100 fluorescence microscope and images obtained with a Hamamatsu C4742-95 camera.

Immunofluorescence of serum-starved mouse C127 cells

For serum starvation experiments, exponentially growing C127 cells were trypsinised, washed twice with DMEM without serum, split 1:3 of their confluent density and cultured on coverslips in the presence of 0.1, 0.2 or 0.4% FBS for 36-48 hours. To estimate the increase of anti-Me(3)K20H4 signal upon serum removal, a number of photographic images were taken at each serum concentration. The brightness of the photographic images was then electronically reduced close to background levels and cells that could still be visualised were counted. At least four fields in three independent experiments for each serum concentration were counted.

Immunolocalisation of Me(3)K20H4 and AcH4 on murine metaphase chromosomes

Unfixed metaphase preparations of C127 mouse mammary tumour cells (ATCC CRL 1616) were labelled by indirect immunofluorescence essentially as published previously (Jeppesen et al., 1992; Jeppesen and Turner, 1993; Cowell et al., 2002). The slides were incubated simultaneously with anti-Me(3)K20H4 antiserum (see above) diluted 1:100, and sheep antiserum S613, raised against a polypeptide consisting of the N-terminal 18 amino acids of histone H4 acetylated at positions serine 1 and lysines 5, 8, 12 and 16 (Morrison and Jeppesen, 2002) diluted 1:800, in KCM (120 mM KCl, 20 mM NaCl, 10 mM Tris-HCl pH 7.5, 0.5 mM EDTA, 0.1% v/v Triton X-100) containing 10% normal horse serum (NHS). Primary antibodies were detected by biotin-conjugated donkey anti-sheep IgG (Sigma product B7390) diluted 1:100, and FITC-conjugated donkey anti-rabbit IgG (Scottish Antibody Production Unit) diluted 1:50, in KCM/10% NHS. TRITC-conjugated Extravidin (Sigma product E3011) diluted 1:100 in KCM/10% NHS was used for visualization of biotin. Images were obtained with a Zeiss Axioskop fluorescence microscope fitted with a Chroma 83,000 triple-band-pass filter set and a Photometrics CH250 CCD camera, using IP Lab Spectrum v3.1 software for capture and analysis.

Immunofluorescence detection of Me(3)K20H4 and sites of DNA synthesis

C127 cells were grown in DMEM supplemented with 10% foetal calf serum and antibiotics. To synchronise cells in S-phase, cells were first synchronised in mitosis as described previously (Gilbert and Cohen, 1987). Selected mitotic cells were plated onto coverslips in fresh medium, and 3 hours later 400 μM mimosine (Sigma) was added to the medium for an additional 10 hours to block cells at the G1/S border (Wu et al., 1997). Cells were then released into S-phase by replacing with warm medium, as previously described (Wu et al., 1997). At various times after release into S-phase, cells were pulse-labelled with 30 μg/ml 5′-bromo-2′-deoxyuridine (BrdU) for 10 minutes and then fixed in 2% paraformaldehyde for 10 minutes at room temperature. Fixed cells were then immunostained as described previously (Cowell et al., 2002). Anti-MeK20H4 antibody was diluted 1:100 and detected by an Alexa 488-conjugated Goat anti-rabbit IgG (Molecular Probes; diluted at 1:200). The bound antibodies were next fixed with 4% formaldehyde in PBS for 15 minutes to preserve them during denaturation and then washed in 0.5% NP40 in PBS for 15 minutes before detection of BrdU according to the method of Wu et al. (Wu et al., 1997). DNA was stained with 10 ng/ml DAPI and cover slips were mounted in Vectashield (Vector Laboratories). Image were obtained with a Nikon Labophot-2 microscope, a 100×, 1.4 NA oil

immersion Nikon Plan Apo objective and a CCD camera (SPOT RT Slider, Diagnostic Instruments, Inc.).

Immunolocalisation of Me(3)K20H4 in surface-spread spermatocytes

Mouse spermatogenic cells were prepared as surface spreads, using the method of Peters et al. (Peters et al., 1997), with some modifications (Cowell et al., 2002). The primary antibodies used were: Guinea pig anti-SCP3 (a gift from R. Benavente) at a dilution 1:500; rabbit anti-Me(3)K20H4 at a dilution 1:1000 and human anti-centromere antibody (ACA) at a dilution of 1:5000. Secondary antibodies used were goat anti-rabbit Cy3 (Amersham Pharmacia Biotech), goat anti-guinea pig Alexa 488 (Molecular Probes) and goat anti-human Cy5 (Amersham Pharmacia Biotech). All secondaries were used at a dilution 1:500.

Slides were subsequently mounted in Vectashield with DAPI (Vector). Where required, controls consisted of omission of primary antibodies and replacement of primary antibodies with pre-immune serum, which resulted in no staining.

Whole-mount immunofluorescent staining of mouse embryos

One-cell embryos were collected from superovulated ($B6C3F_1 \times$ C57Bl/6) female mice, as previously described (Pratt, 2001). Embryo culture was performed in M16 medium (Sigma) at 37°C in a humidified atmosphere containing 5% CO_2. Two- to four-cell embryos were flushed out of the oviducts 48 hours and 53 hours post-HCG, respectively, and washed in M2 medium (Sigma).

The embryos were fixed for 30 minutes in 2% (v/v) formaldehyde in PBS, and then immunostained essentially as described previously (Cowell et al., 2002). Anti-Me(3)K20H4 was used in 1:500 dilution at 37°C for 1 hour and was detected with anti-rabbit immunoglobulins/FITC (DAKO F0205) at a dilution 1:20. The embryos were mounted in mounting medium containing 1.5 μg/ml DAPI (Vector H-1200). Fluorescence was detected with a Zeiss fluorescence microscope, using filter combinations suitable for the different fluorochromes.

Staining of *Drosophila* polytene chromosomes

Me(3)K20H4 was detected by immunostaining of polytene chromosomes of the wild-type Oregon-R stock with the anti-Me(3)K20H4 rabbit antibody (1:50 dilution). The immunostaining was performed according to the method of James et al. (James et al., 1989). An anti-rabbit Cy3-linked (Jackson) secondary antibody was used. The slides were incubated in 0.05 μg/ml of DAPI dissolved in 2× SSC for 4 minutes and mounted in antifading solution. Chromosome preparations were analysed using a computer-controlled NIKON E 1000 epifluorescence microscope equipped with a cooled CCD camera (Coolsnap). Using the Adobe Photoshop program, the fluorescent signals, recorded separately as grey scale digital images, were pseudocoloured and merged.

Immunolocalisation of Me(3)K20H4 on mealy bug chromosomes

Chromosome spreads on slides were prepared as previously described (Bongiorni et al., 1999; Bongiorni et al., 2001; Cowell et al., 2002). Anti-Me(3)K20H4 diluted 1:300, was applied overnight, at 4°C and detected with a goat anti-rabbit IgG (H+L) conjugated with Alexa™ 594, diluted 1:600. The spreads were counterstained with 0.2 μg/ml DAPI (Boehringer-Mannheim) in 2× SSC for 5 minutes and mounted in antifade solution (Dabco, Sigma). Immunofluorescent preparations were observed and documented as previously described (Cowell et al., 2002), using filter combinations suitable for the different fluorochromes.

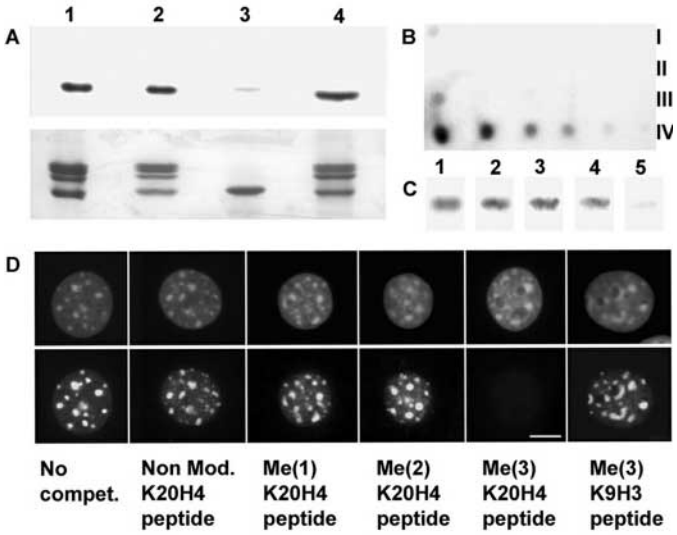

Fig. 1. Specificity of the antibody for *tri*-methylated lysine 20 of histone H4 (anti-Me(3)K20H4). (A) The anti-Me(3)K20H4 antibody recognises methylated H4 by western blotting. Histones from various sources were separated by SDS-PAGE, blotted and probed with anti-Me(3)K20H4. The sources of the histones were: turkey erythrocyte nuclei (lane 1), turkey erythrocyte core histones (lane 2), recombinant H4 (lane 3) and calf thymus core histones (lane 4). The bottom row shows a Coomassie Blue-stained profile of the samples used in the immunoblot. (B) Specificity of anti-Me(3)K20H4 antibody for the trimethylated form of K20 as determined by dot blotting. Serial dilutions (lanes left to right) of the non modified (I), mono- (II), di- (III) and tri-methylated (IV) K20 peptides were dot blotted onto nitrocellulose and then probed with anti-Me(3)K20H4. (C) The antibody is specific for Me(3)K20H4 in a competition assay using specific methylated peptides and membrane-bound histone H4. Calf thymus histone H4 is identified on an immunoblot by the anti-Me(3)K20H4 antibody alone (lane 1) or preincubated with non modified (lane 2), Me(1)K20H4 peptide (lane 3) and Me(2)K20H4 peptide (lane 4). Preincubation of the antibody with the Me(3)K20H4 peptide abolishes binding to H4 histone (lane 5). (D) The antibody is specific for Me(3)K20H4 in a competition assay using immunofluorescence (bottom row; top row are the corresponding DAPI profiles). From left to right: no competitor, non modified K20H4 peptide, Me(1)K20H4 peptide, Me(2)K20H4 peptide, Me(3)K20H4 peptide. In the last panel a Me(3)K9H3 was used as a competitor. Only the Me(3)K20H4 peptide competes. Scale bar: 5 μm.

Results

Authentication of the anti-Me(3)K20H4 antiserum

In order to detect Me(3)K20H4 in chromosomal DNA we raised a specific rabbit antibody to *tri*-methylated lysine 20 of histone H4 (see Materials and Methods). Immunoblotting (Fig. 1A) showed that the antibody recognises histone H4 in turkey erythrocyte nuclei (lane 1), turkey erythrocyte core histones (lane 2) and commercially available calf thymus core histones (lane 4) and has negligible reactivity to recombinant H4 histone (lane 3). We also checked for possible cross reactivity on the non-modified H4 peptide and with mono- or di-methylated K20H4 peptides. Accordingly, serial two-fold dilutions of the non modified (Fig. 1B, row I), mono-methylated (row II), di-methylated (row III) and tri-methylated H4 peptides (row IV), were spotted onto nitrocellulose and probed with the anti-serum. As shown in Fig. 1B, the antibody activity is almost

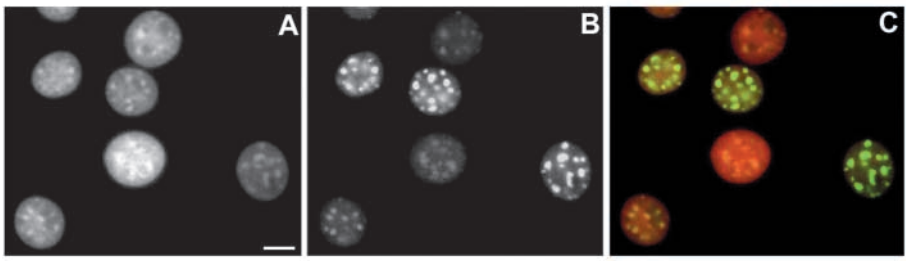

Fig. 2. Distribution of Me(3)K20H4 in an asynchronous population of C127 mouse cells. (A) The DAPI profile of C127 cells. (B) The same field as in A stained for the Me(3)K20H4. (C) The merged image of A and B; DAPI is pseudocoloured in red and Me(3)K20H4 in green. Scale bar: 5 μm.

exclusively directed against the *tri*-methylated H4 peptide. To confirm that the signal in the 'dot-blot' (Fig. 1B) is derived from the antibodies in the serum that are directed to the *tri*-methylated K20H4, we undertook a competition assay using, as competitors, non-modified, mono-, di- and tri-methylated H4 peptides (Fig. 1C). Fig. 1C shows calf thymus H4 probed with the antibody alone (lane 1) or probed with antibody and either the non-modified (lane 2), mono- (lane 3), di- (lane 4) and tri-methylated (lane 5) K20 histone H4 peptide. Only the tri-methylated peptide has the ability to act as a competitor eliminating the H4 signal.

Finally, the specificity of the antibody was again confirmed by immunostaining cells with either the antibody alone or with antibody incubated in the presence of competitor peptides, as for the immunoblotting experiment depicted in Fig. 1C. Staining of C127 mouse mammary tumour cells, which have characteristic DAPI-positive blocks of heterochromatin (Fig. 1D, upper row), showed that Me(3)K20H4 has a heterochromatic distribution (panel on left of lower row, Fig. 1D). This heterochromatic signal is completely abolished by the *tri*-methylated K20H4 peptide and is not affected by any of the other competitor H4 peptides or by a histone H3 peptide *tri*-methylated at lysine 9.

Me(3)K20H4 localises to constitutive heterochromatin during interphase and at metaphase in mouse cells

Having established the specificity of anti-Me(3)K20H4 antibody, we investigated the distribution of Me(3)K20H4 during interphase and on metaphase chromosomes by indirect immunofluorescence (Figs 2, 3). When we stained an asynchronous population of C127 cells, with the anti-Me(3)K20H4 we could show that the antibody localised to DAPI-positive heterochromatic blocks (Fig. 2). The immunostaining also revealed that the levels of the labelling varied, from cell-to-cell, going from heavily decorated, to an intermediate level of staining, to cells that exhibit very weak fluorescence signals. This variability indicates that *tri*-methylation of K20 on H4 may be cell cycle regulated.

The distribution of Me(3)K20H4 at metaphase was determined by staining C127 metaphase chromosome spreads with the anti-Me(3)K20H4 antibody. As shown, Me(3)K20H4 is concentrated within centromeric heterochromatin (Fig. 3). At higher magnification (see inset of Fig. 3) the Me(3)K20H4 staining appears 'punctate' indicating that Me(3)K20H4 may not be uniformly distributed throughout centromeric heterochromatin during metaphase, but rather that Me(3)K20H4 could define a specific type of domain within constitutive heterochromatin. The C127 cell line is female and contains an inactive X chromosome, which allowed us to investigate whether Me(3)K20H4 was enriched on the X_i. We found that, apart from centromere, the inactive X chromosome, as defined by the characteristic lack of AcH4, is not stained (arrow in Fig. 3), indicating that Me(3)K20H4 is unlikely to be involved in facultative heterochromatinisation of the X_i.

Me(3)K20H4 is a component of the late replicating chromatin

One of the characteristic hallmarks of heterochromatin, be it constitutive or facultative, is that it replicates late during S-phase of the cell cycle. The localisation of Me(3)K20H4 to

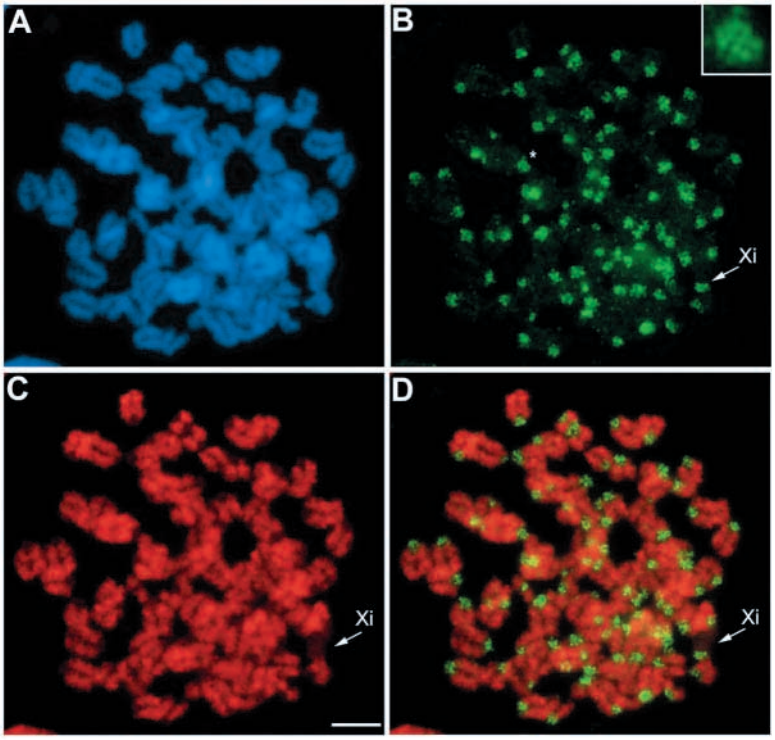

Fig. 3. Distribution of Me(3)K20H4 in murine metaphase chromosomes. (A) DAPI profile of the chromosome-spread from a mouse C127 cell. (B) The spread in A labelled with anti-Me(3)K20H4, which shows labelling of peri-centromeric heterochromatin. The labelling is punctate, as seen in the inset, which is a magnified image of the centromeric Me(3)K20H4 staining indicated by the asterisk. (C) The spread in A labelled with anti-AcH4 antibody. (D) The merged image of B and C. Arrows in B,C and D point to the inactive X chromosome (Xi), which is underacetylated in C. Scale bar: 5 μm.

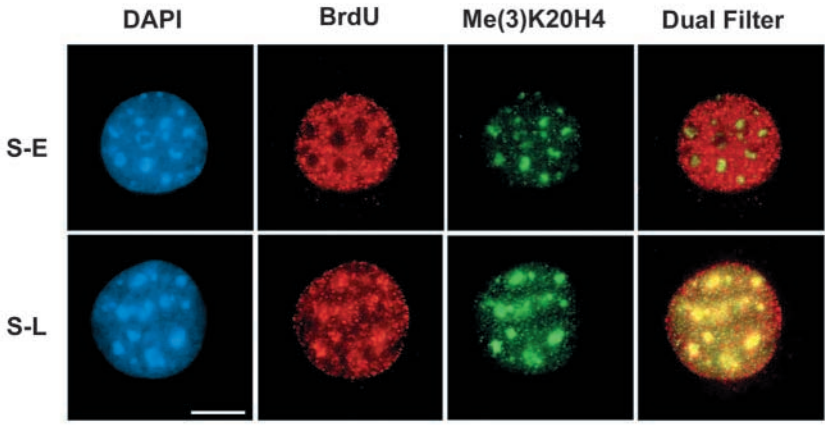

Fig. 4. Me(3)K20H4 replicates late in S-phase of the cell cycle. C127 cells were arrested at the G1/S border with mimosine and then released into S-phase. Cells were pulse labelled with BrdU either early (2 hours after release, S-E) or late (8 hours after release; S-L) in S-phase, and were then stained for DAPI (blue), BrdU (red) and Me(3)K20H4 (green). In the far right column, the BrdU and Me(3)K20H4 staining patterns were simultaneously visualised through a dual FITC/Texas Red filter (Dual Filter). This showed that the BrdU and Me(3)K20H4 staining patterns colocalise late in S-phase (S-L). Scale bar: 5 μm.

heterochromatic blocks prompted us to see if Me(3)K20H4 marked chromatin replicated late in S-phase. Accordingly, we determined the time at which chromatin labelled with Me(3)K20H4 replicates using dual labelling with BrdU and anti-Me(3)K20H4 antibodies. As shown in Fig. 4, cells pulse-labelled with BrdU late in S-phase (S-L; 8 hours post-release from mimosine block) showed colocalisation of BrdU with Me(3)K20H4 antibodies, confirming that Me(3)K20H4-enriched chromatin replicates late in S-phase. No overlap between BrdU staining and Me(3)K20H4 staining was observed at early S-phase (S-E; 1 hour post release).

The levels of Me(3)K20H4 are raised in serum-starved cells

Recent mass spectroscopy studies indicate that Me(3)K20H4 levels increase in mammalian cells as the cells are induced into stationary (G0) phase (Sarg et al., 2002). To see if we could detect such a change using our antibody, we determined levels of Me(3)K20H4 in serum-starved cells. As described earlier (Fig. 2) there is a considerable variation in the levels of Me(3)K20H4 staining (Fig. 5A), with a few cells showing brightly staining blocks of Me(3)K20H4 that are precisely co-incident with the DAPI-bright heterochromatic regions found in close juxtaposition to the nucleoli (a magnified image of a brightly stained nucleus is given in Fig. 5G). We found that both the general levels of staining and the number of brightly stained nuclei increased when we reduced the levels of the serum in the culture media from 10% to 0.4% (Fig. 5C). The staining was enhanced even more when the serum levels were further reduced to 0.1% (Fig. 5E). To estimate this increase in staining we counted the number of relatively brighter cells at each serum concentration (see Materials and Methods). In normal culture medium these cells were approximately 10% of the total population. This percentage increased to between 40 to 50% and 80 to 90% at serum concentrations of 0.4 and 0.1%, respectively. Thus, the data indicate that K20H4 *tri*-methylase activity is increased as cells are induced into a stationary phase by serum starvation.

Me(3)K20H4 localise to centromeric heterochromatin, the pseudoautosomal region (PAR) and a few telomeres during spermatogenesis

The lack of Me(3)K20H4 on the facultative heterochromatin of X_i (see Fig. 3) prompted us to investigate the distribution of Me(3)K20H4 during pachytene/diplotene stages of male meiosis where the X chromosome undergoes an analogous process of facultative heterochromatinisation in the XY-body (Solari, 1974). To substage meiosis, we used an antiserum to the axial

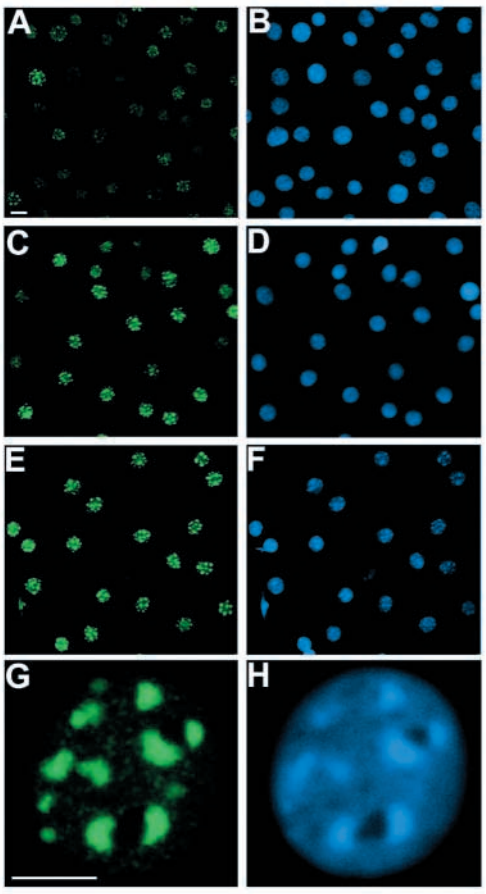

Fig. 5. Decoration of DAPI-positive heterochromatin blocks with anti-Me(3)K20H4 antibody in C127 cells is enhanced upon serum removal. C127 cells were cultured in normal culture medium (A,B) or in culture medium containing 0.4% (C,D) and 0.1% (E,F) foetal calf serum. (A,C,E,G) Staining with anti-Me(3)K20H4; (B,D,F,H) DAPI profiles of the same fields. One heavily decorated nucleus, typically found in cells cultured in low serum concentration, is shown in G and H. Scale bars: 10 μm (A-F); 5 μm (G,H)

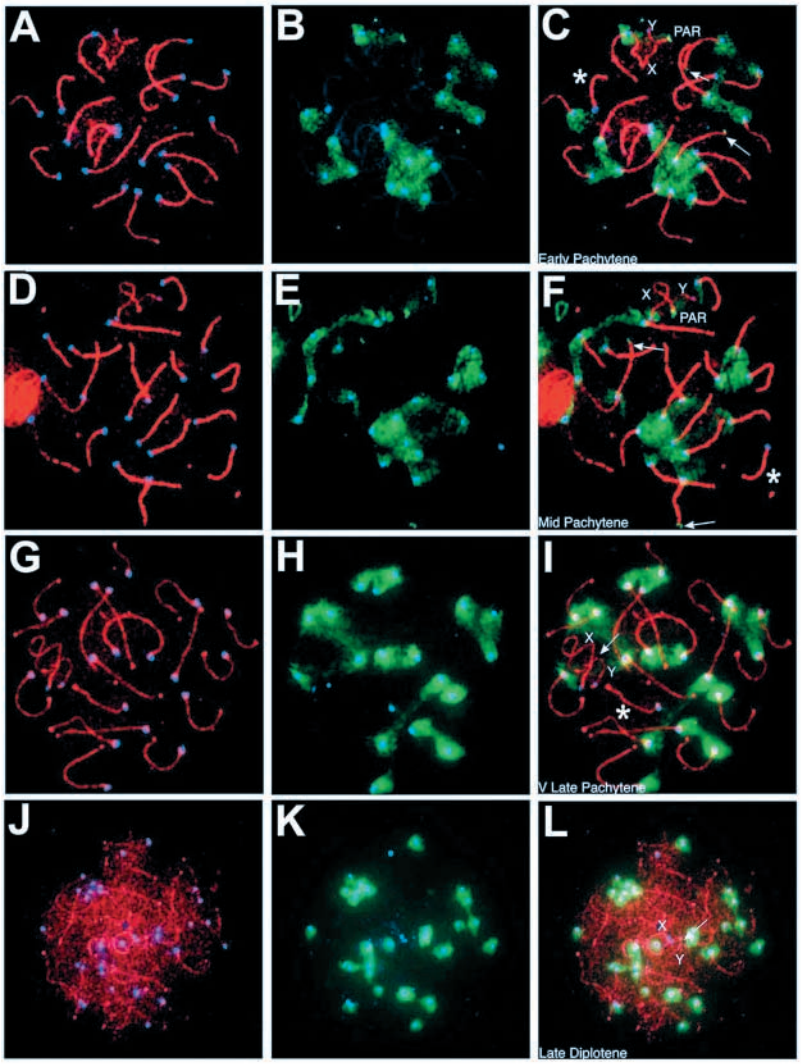

Fig. 6. Me(3)K20H4 localises to the centromeric and telomeric heterochromatin during spermatogenesis and transiently accumulates at the PAR region. Me(3)K20H4 distribution (green) is followed in pachytene and diplotene nuclei. The axial elements of the paired chromosomes are visualised with anti-SYCP3 antibodies (red) and the centromeres with human anti-centromeric antibodies (ACA; blue). During early (A-C) and mid-pachytene (D-F), Me(3)K20H4 localises at the centromeres, some of the telomeres (arrows in C and F) and the PAR region of the XY-body. The centromeric heterochromatin of one of the autosomes (asterisk) and of the Y chromosome are not stained with anti Me(3)K20H4 antibodies. At late pachytene (G-I) and diplotene (J-L) the PAR (arrow indicates the PAR) and telomeric staining of Me(3)K20H4 have disappeared.

element protein SYCP3 (von Glasenapp and Benavente, 2000), which stains the axes of the chromosomes red (Fig. 6).

During early prophase I, leptotene and zygotene, Me(3)K20H4 staining of nuclei is weak but localises to DAPI-positive blocks of constitutive heterochromatin (data not shown). As cells enter early pachytene, paired homologues show an intense Me(3)K20H4 staining (FITC; green) around most centromeres, as defined by an anti-ACA serum (ACA is the blue signal in Fig. 6). There is, however, one centromere of an autosomal bivalent that remains unstained (asterisk in Fig. 6C). Indeed, at all stages depicted in Fig. 6 there is one autosome (bivalent) that remains negative for Me(3)K20H4 (labelled with an asterisk). Whether it is the same chromosome, which seems most likely, is not known. Me(3)K20H4 is not localised to the centromeric heterochromatin of the Y chromosome at any stage, indicating that Me(3)K20H4 may be targeted to major satellite DNA, which is absent from the Y centromere (Pardue and Gall, 1970). We also see staining of few telomeres (arrows in Fig. 6C). Most strikingly, we see that Me(3)K20H4 localises to the distal region of the XY-synapsis, also known as the pseudoautosomal region (PAR). This PAR focus appears at the same time as the HP1β and Me(3)K9H3 PAR foci (Turner et al., 2001; Peters et al., 2001).

A similar Me(3)K20H4 staining pattern is observed during mid-pachytene where the centromeres of all autosomes, except one (asterisk), are stained with the Me(3)K20H4 antibody (Fig. 6F). Some telomeres still have a distinct Me(3)K20H4 signal (arrow in Fig. 6F), and the Me(3)K20H4 PAR focus is also present. However, the Me(3)K9H3 staining observed over the XY-body at this time (Cowell et al., 2002; Peters et al., 2001), is not observed for Me(3)K20H4.

At very late pachytene the centromeric staining remains on all autosomes except one, but both the telomeric and PAR focus have disappeared (Fig. 6G-I; arrow points to PAR). It is interesting to note that this is the time when HP1β accumulation, which follows Me(3)K9H3, is first seen over the XY-body (Turner et al., 2001; Cowell et al., 2002). Thus HP1 accumulation at the XY-body follows Me(3)K9H3 and does not appear to require Me(3)K20H4. At late dipolotene (Fig. 6J-L) the pattern of Me(3)K20H4 staining is the same as that seen at very late pachytene.

In a final experiment we stained mature spermatozoa (Fig. 7A-C) with the anti-Me(3)K20H4 antibody and showed that mature sperm contain very low, but detectable, levels of Me(3)K20H4 (Fig. 7B), which colocalises with the DAPI-positive blocks of constitutive heterochromatin (Fig. 7A and merged image in Fig. 7C).

Me(3)K20H4 is depleted in the paternal pronucleus and both parental genomes gradually become depleted in Me(3)K20H4 by the two-cell stage

Guided by the observation that mature spermatozoa contain Me(3)K20H4 (Fig. 7), we next investigated the distribution of Me(3)K20H4 in the unfertilised oocyte. We also studied the distribution of Me(3)K20H4 during fertilisation, pronuclei formation and the early cleavage divisions. The maternal (ma) chromosomes in a MII-arrested oocyte stain strongly for Me(3)K20H4 (Fig. 8A-C). Immediately after fertilisation, the spermatozoon (sp) can be observed as a DAPI-stained crescent at the periphery of the oocyte (bottom of Fig. 8D); the maternal chromosomes are still at metaphase II. The sperm appears to contain no immunocytologically detectable Me(3)K20H4, while Me(3)K20H4 is present within the polar body (pb) and

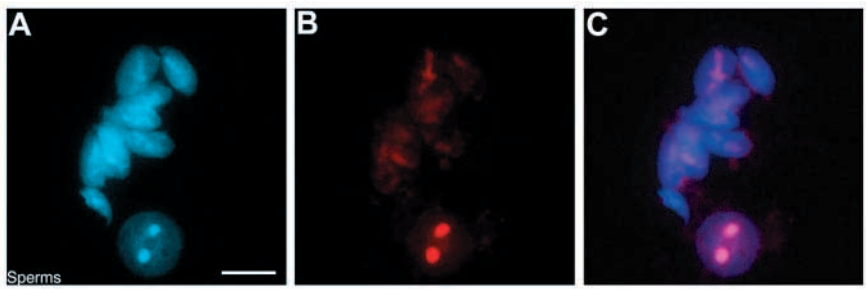

Fig. 7. Me(3)K20H4 is present in mature sperm. Hypotonically swollen sperm stained with DAPI (A) and anti-Me(3)K20H4 antibodies (B). (C) Merged image of A and B. Me(3)K20H4 staining colocalises with the bright (AT-rich) DAPI staining blocks. Me(3)K20H4 staining of the sperm is weak; when compared to the single spermatid, below the sperm cells (the 'double-dot' staining), the intensity of the Me(3)K20H4 staining in the sperm cells is weak, but detectable. Scale bar: 5 μm.

the maternal chromosomes (Fig. 8E,F). One possibility was that the absence of (Me(3)K20H4 in the fertilising spermatozoon was an artefact resulting from antibody exclusion or to the slightly different fixation conditions used for surface spread sperm (Fig. 7; see Materials and Methods), which results in the loss of the Me(3)K20H4 epitope. However, we were dissuaded from this interpretation because: (i) the Me(3)K20H4 is still detectable in the condensed metaphase II maternal chromosomes and, (ii) we examined many stages, from sperm entry through sperm head decondensation to the formation of a well-defined pronucleus, and found that the paternal chromosomes always lacked detectable Me(3)K20H4. An example is given in Fig. 8G-I, where the somewhat larger paternal (pa) pronucleus does not contain detectable Me(3)K20H4, while the heterochromatin surrounding the nucleoli in the smaller maternal (ma) pronucleus is clearly stained with anti-Me(3)K20H4. Thus, in the same environment, under the same fixation conditions, the parental pronuclei exhibit a striking non-equivalence in terms of Me(3)K20H4.

The difference in parental Me(3)K20H4 levels is also observed at subsequent stages of development. It is very clear at syngamy, which is the stage at which the parental chromosomes condense and come together to form a unique metaphase plate, just before the embryo cleaves to form two cells. At syngamy, the paternal chromosome set, which has undergone DNA replication and is now diploid, is devoid of Me(3)K20H4, while the centromeric heterochromatin within the diploid maternal set is clearly labelled with the anti-Me(3)K20H4 antibody (Fig. 8J-L). After the first mitosis, the difference between the parental chromosomes can also be observed in the two-cell embryo; each cell contains a diploid nucleus with a set of maternal and paternal chromosomes. As

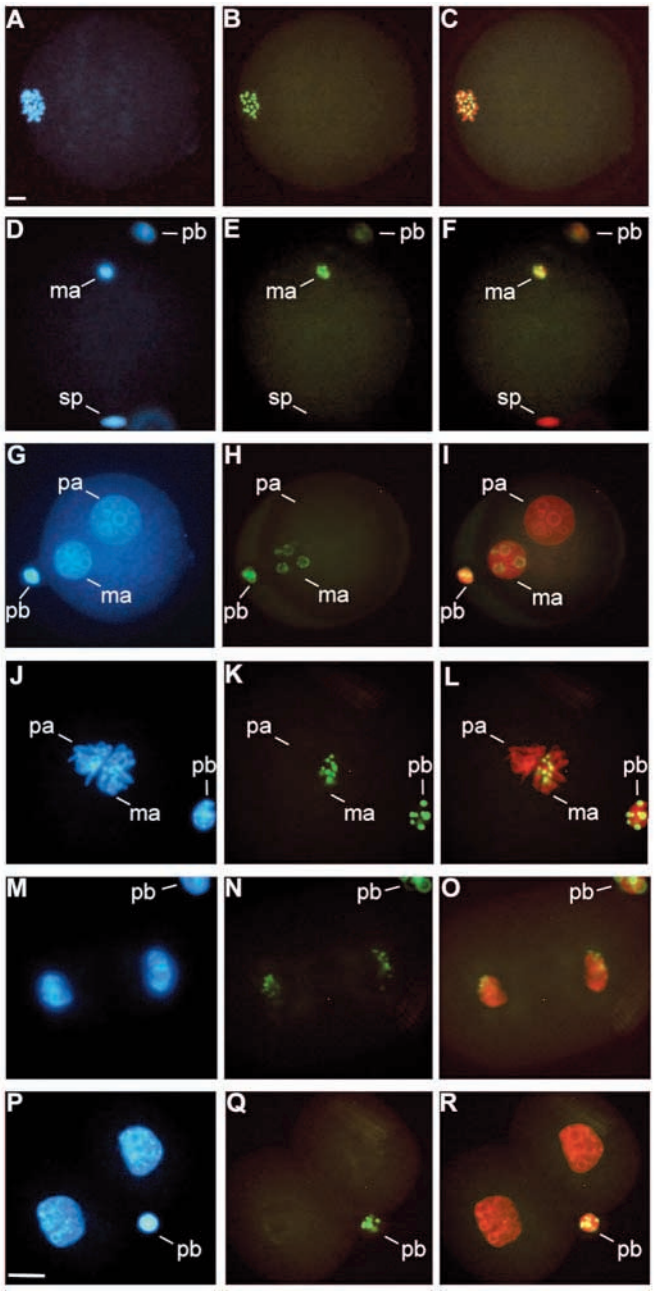

Fig. 8. Distribution of Me(3)K20H4 in oocytes and one- and two-cell mouse embryos. (A,D,G,J,M,P) Oocytes and one- and two-cell embryos stained with DAPI. The sperm (sp), maternal (ma), paternal (pa) and polar body (pb) DNA stains intensely with DAPI compared with the cytoplasm. (B,E,H,K,N,Q) The same embryos were stained using the anti-Me(3)K20H4 antibody and the immunofluorescence (FITC) is shown in green. (C,F,I,L,O,R) Merged images of the embryos in the left and the middle columns. DAPI is pseudocoloured in red; colocalisation is yellow. (A-C) Me(3)K20H4 is enriched in the maternal centromeres of a metaphase II-arrested oocyte. (D-F) Approximately 1 hour after fertilisation (n=10) the sperm nucleus is found in the ooplasm and lacks Me(3)K20H4, while the polar body and the maternal chromosomes contain Me(3)K20H4. (G-I) Me(3)K20H4 is present in the maternal pronucleus but undetectable in the paternal pronucleus (pronuclear stage: n=32). (J-L) At syngamy (n=33) the difference in Me(3)K20H4 between the parental chromosomes is clear. (M-O) Me(3)K20H4 staining is partitioned in the late telophase/early G1 phase two-cell embryo (early two cell; n=15). (P-R) At late two-cell embryos (n=35) the intensity of Me(3)k20H4 staining is very weak. Scale bars: 10 μm (A-L); 10 μm (M-R).

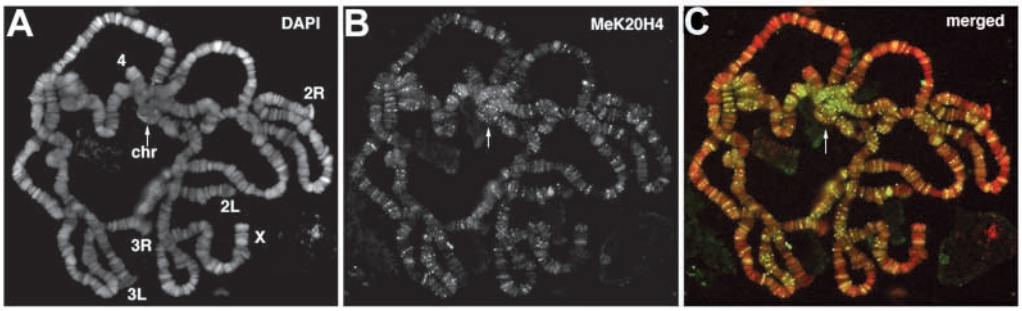

Fig. 9. Me(3)K20H4 distribution on *Drosophila* polytene chromosomes. A polytene chromosome spread stained with DAPI (A) and anti-Me(3)K20H4 (B). (C) Merged image of A and B. Me(3)K20H4 has a punctate appearance and is concentrated at the chromocenter (arrow) and at numerous euchromatic bands.

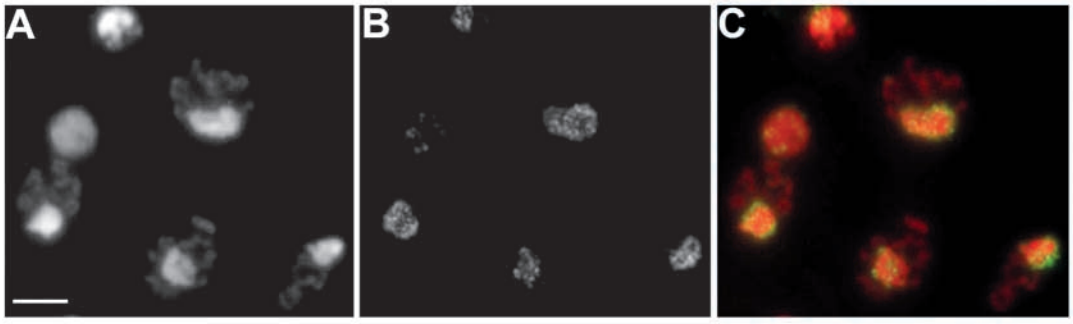

Fig. 10. Me(3)K20H4 is present only at the paternal chromosomes of male mealy bugs. Prometaphase male mealy bug cells stained with DAPI (A) and anti-Me(3)K20H4 (B). (C) Merged image of A and B. Me(3)K20H4 (green) has a punctate appearance and is distributed through the paternal chromosome set, which stains intensely with DAPI (pseudocoloured in red). Scale bar: 5 μm.

seen, Me(3)K20H4 localises to a portion of the reforming early-G1 nuclei (Fig. 8M-O; especially the merged image in 8O). Because it is the maternal chromosomes that are stained in all previous stages we suspect that the Me(3)K20H4 is preferentially associated with the maternal chromosome set. After this early G1 staining pattern we find that there is a reduction in Me(3)K20H4 staining intensity in two-cell stage embryos (Fig. 8P-R). This lower level of staining remains until the blastocyst stage of development (data not shown).

Me(3)K20H4 distribution on *Drosophila* polytene chromosomes

We next investigated the distribution of Me(3)K20H4 in *Drosophila* polytene chromosomes which give a much higher resolution than that obtainable with mammalian chromosomes. Staining of polytene chromosomes revealed that Me(3)K20H4 is found diffusely through the chromocenter, with small speckles of higher concentration which give a punctate appearance (arrow in Fig. 9). Me(3)K20H4 is also found at many euchromatic bands and, again the pattern is punctate and, at many sites, does not extend uniformly across the bands. To confirm the above distribution we applied different protocols and we obtained consistent results (data not shown). However, the possibility that the observed patterns depend on the technical procedure or the nature of the antibody used cannot be excluded.

Me(3)K20H and parental imprinting in mealy bugs

In order to address the role of Me(3)K20H4 in imprinting we stained chromosomes in male mealy bugs. Cellular suspensions of embryonic tissues were prepared by dissection of gravid females. Both male and female embryonic cells are present in these preparations, but the male tissues can be clearly distinguished by DAPI staining; the heterochromatic chromosomes form a brightly stained chromocenter (Fig. 10A-C) (Epstein et al., 1992; Bongiorni et al., 1999; Bongiorni et al., 2001). When male prometaphase cells were stained with the anti-Me(3)K20H4 antibody the signal was over the paternal chromosome set. Of interest is that the staining pattern is punctate, much like that seen at the chromocenter of *Drosophila* polytene chromosomes and the staining seen at the mouse centromeres at metaphase (Fig. 9).

In female mealy bug cells Me(3)K20H4 is found scattered throughout the chromosomes; no differences were seen between the homologous chromosomes (data not shown).

Me(3)K20H4 is dependent upon Suv3(9)h1/h2 H3-specific HMTase activity

We have previously shown that Me(3)K9H3 is associated with constitutive heterochromatin (Cowell et al., 2002). Here we show that Me(3)K20H4 also localises to constitutive heterochromatin in mammals – the X_i is not decorated by the anti-Me(3)K20H4 antibody (Fig. 3). Localisation to constitutive heterochromatin is therefore a characteristic shared by both Me(3)K20H4 and Me(3)K9H3 and, because of this, we wondered whether the regulation of these two histone modifications was also linked. To address this question, we used an immortalised embryonic fibroblast cell line, which lacks any

functional Suv3-9 HMTase activity (Peters et al., 2002). In this cell line Me(3)K9H3 is not enriched within centromeric heterochromatin, but is dispersed in the nucleoplasm in a fine speckled pattern (data not shown). Staining with the anti-Me(3)K20H4 antibody revealed that the Me(3)K20H4 is also dispersed through the nucleoplasm in interphase cells (Fig. 11A-C). Also, at metaphase, no reproducible Me(3)K20H4 signal is seen at the centromeres in Suv3-9 null cells (Fig. 11D). By contrast, in wild-type cells with intact Suv3-9 activity, the typical, albeit variable, Me(3)K20H4 staining is observed at the DAPI-positive heterochromatic blocks (Fig. 11E-G) and a robust Me(3)K20H4 signal is seen at the centromeres in cells at metaphase (Fig. 11H). These data indicate that the localisation of Me(3)K20H4 is regulated by Suv3-9h1/h2 activity and that the dominant histone modification is Me(3)K9H3.

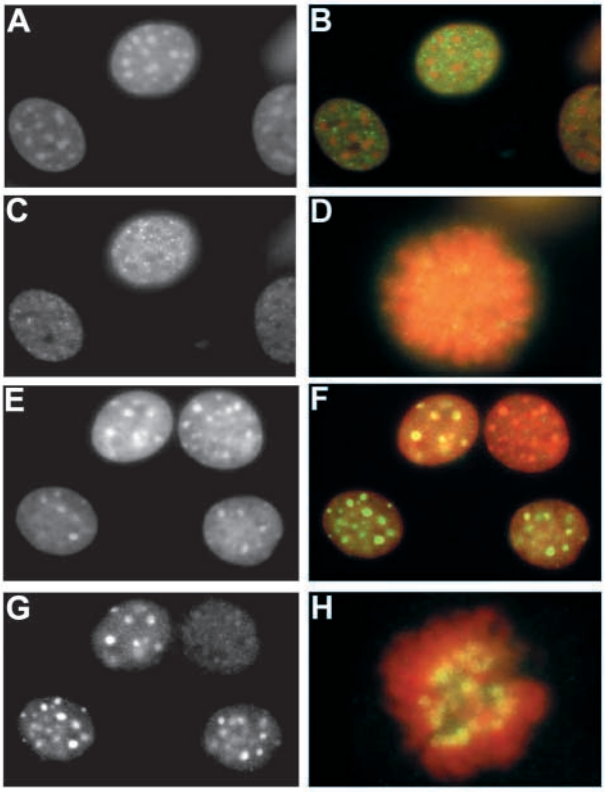

Fig. 11. Distribution of Me(3)K20H4 is dependent upon Suv 3(9)h1/h2 H3-specific HMTase activity. B is the merged image of A and C, and F is the merged image of E and G; DAPI is pseudocoloured red and Me(3)K20H4 green. Staining of Suv3-9 null cells with the anti-Me(3)K20H4 antibody shows that Me(3)K20H4 is distributed throughout the nucleoplasm (C), outside the DAPI-positive blocks of constitutive heterochromatin (A; merged image in B). In a mitotic nucleus from the Suv3-9 null cell line the Me(3)K20H4 is absent from centromeric heterochromatin (D). This is in stark contrast to a mitotic cell from wild-type mouse fibroblasts (H), where there is robust staining of the centromeric heterochromatin. In an asynchronous population of wild type cells, the staining of Me(3)K20H4 is variable (G), as previously described (see Figs 2 and 5), and present over the DAPI-positive blocks of heterochromatin (E; merged image in F).

Discussion

Immunofluorescence using an antibody specific for Me(3)K20H4 has shown that constitutive heterochromatin (at the centromeres and telomeres) in mammalian cells is enriched in Me(3)K20H4 (Figs 3, 6). This is distinct from Me(3)K9H3, which has a broader distribution; Me(3)K9H3 is found at the centromeres, as well as in a G-band-like pattern along the chromosome arms and is also present along the length of the facultatively heterochromatinised X_i in female cells (Cowell et al., 2002). However, chromatin enriched in both Me(3)K9H3 and Me(3)K20H4 replicates late during the S-phase of the cell cycle, which is a classic hallmark of heterochromatin (Fig. 4).

In an asynchronous population of cells the levels of Me(3)K20H4 vary greatly indicating that the K20H4 trimethylase activity may change according to cell cycle stage (Fig. 2, Fig. 5A). Our own observation that serum starvation to induce a G0-like stage results in an increase in Me(3)K20H4 levels at constitutive heterochromatin, would support regulation of K20 trimethylase activity (Fig. 6). An increase in Me(3)K20H4 in cells in stationary phase has previously been observed using mass spectrometric analysis of chromatographically separated forms of methylated K20H4 (Sarg et al., 2002).

Me(3)K20H4 in relation to facultative heterochromatinisation and parental imprinting

We have not found Me(3)K20H4 enriched within the facultatively heterochromatinised X_i (Figs 3, 5). Nor is it enriched in the XY-body during mammalian spermatogenesis (Fig. 6). These data indicate that Me(3)K20H4 is unlikely to be required for facultative heterochromatinisation in mammals. However, staining of the paternal chromosome set in mealy bugs (Fig. 10) indicates that Me(3)K20H4 may have a role in the process of facultative heterochromatinisation and imprinting that is found in this organism. It is an open question as to whether mammalian imprinted genes, which lie within similar repressed chromosomal domains (Banerjee et al., 2000), are enriched in Me(3)K20H4.

The punctate distribution of Me(3)K20H4 in heterochromatin

One of the features found in several chromosome preparations, including centromeric heterochromatin in metaphase chromosomes (Fig. 3; especially the inset), the paternal chromosome set in mealy bugs (Fig. 10) and the chromocenter in *Drosophila* polytene chromosomes (Fig. 9) is that Me(3)K20H4 is found in a punctate pattern. It has been known for many years, from elegant genetical analyses in *Drosophila*, that heterochromatin is made up of distinct domains containing different combinations of protein components, some of which are shared between domains and others that are unique to one domain or other (reviewed by Singh and Huskisson, 1998). We suggest that the punctate pattern we see for Me(3)K20H4 may identify a biochemically distinct domain within cytologically defined heterochromatin. In the case of mouse metaphase cells the pattern is likely to represent a type of domain that is heavily represented in centromeric heterochromatin. This could be a major satellite sequence in mouse heterochromatin and would be consistent with our observation that Me(3)K20H4 is absent from the Y centromere (Fig. 6), which lacks major satellite

sequences found on the autosomal centromeres (Pardue and Gall, 1970).

The observation that Me(3)K20H4 is found at many bands on polytene chromosomes is in line with the finding that Me(3)K20H4 exists in *Drosophila* (Starbuck et al., 1968) and complements the observation that Me(2)K20H4 is also found at many bands (Nishioka et al., 2002; Fang et al., 2002). As with Me(2)K20H4 we suggest Me(3)K20H4-positive bands represent repressed chromosomal domains.

However the Me(3)K20H4 (Fig. 9) and the Me(2)K20H4 staining patterns differ in that the Me(3)K20H4 pattern is again punctate and does not extend across the bands at many sites (Fig. 9). One possible explanation for this 'unusual' pattern is that trimethylation activity is very low in early stages of development. It is known that in mammals the Me(3)K20H4 gradually increases with ageing (Sarg et al., 2002). Because the fly maggot is a larva, reduced levels of K20H4 trimethylase activity at this early stage of development might lead to incomplete trimethylation of individual chromomeres of each chromonemata, resulting in the observed punctate pattern of bands along the polytene chromosome arms.

Distribution of Me(3)K20H4 during mouse embryogenesis

We have shown that mature sperm contain detectable levels of Me(3)K20H4 (Fig. 7). However, an hour after fertilisation Me(3)K20H4 cannot be detected in the fertilising spermatozoon (Fig. 8D-F). The absence of detectable Me(3)K20H4 in the newly fertilised egg may result from additional histone modification(s) that block reactivity of our antibody to Me(3)K20H4 or from Me(3)K20H4 associated with mature sperm (Fig. 7), being removed by activities in the oocyte cytoplasm. Such activities could involve specific histone demethylases, histone replacement mechanisms or proteolytic enzymes that degrade Me(3)K20H4.

The removal and consequent lack of Me(3)K20H4 within the paternal pronucleus (Fig. 8D-L), which is followed by a reduction to barely detectable levels of Me(3)K20H4 by the late two-cell stage (Fig. 8M-R) is intriguing because it follows the pattern of 5-methylcytosine (MeC) demethylation during mouse embryogenesis (Monk et al., 1987; Kafri et al., 1993). The pace of MeC demethylation is different for each parental genome. The MeCs in the paternal chromosomes are actively demethylated and this active demethylation begins at around 6 hours after fertilisation – by 8 hours the paternal chromosomes are much depleted in MeC (Mayer et al., 2000). By contrast, demethylation of MeC in the maternal chromosomes occurs by a passive, replication-dependent mechanism (Bouniol-Baly et al., 1997), and it takes two cleavage divisions before the MeC levels in the parental chromosomes are at an equivalent, albeit depleted, level (Mayer et al., 2000; Oswald et al., 2000). Our results indicate that active MeC demethylation, either by specific demethylases or by excision repair mechanisms, could be mechanistically related to the mechanism underlying Me(3)K20H4 demethylation described in this work (Fig. 8).

Me(3)K20H4 localisation is dependent upon Suv(3)9h1/h2 activity

On a genetic background where both Suv(3)9h1 and Suv(3)9h2 functions have been abrogated we find that the localisation of Me(3)K20H4 is disturbed. Instead of being enriched in blocks of constitutive heterochromatin Me(3)K20H4 is distributed in a 'fine-grain' pattern throughout euchromatin (Fig. 11A-D). The dependence of Me(3)K20H4 on Suv(3)9h1/h2 H3 methyltransferase activity, and by extension, Me(3)K9H3, indicates that Me(3)K20H4 and Me(3)K9H3 epigenetic 'marks' are related and could be involved in the regulation of peri-centromeric heterochromatin structure. Our current work is directed towards testing this hypothesis.

Dr Kourmouli is a recipient of an EMBO Long Term Fellowship. Work in the Singh Laboratory is funded by a BBSRC Core Strategic Grant.

References

Banerjee, S., Singh, P. B., Rasberry, C. and Cattanach, B. M. (2000). Embryonic inheritance of the chromatin organisation of the imprinted H19 domain in mouse spermatozoa. *Mech. Dev.* **90**, 217-226.

Bannister, A. J., Zegerman, P., Partridge, J. F., Miska, E. A., Thomas, J. O., Allshire, R. C. and Kouzarides, T. (2001). Selective recognition of methylated lysine 9 on histone H3 by the HP1 chromo domain. *Nature* **410**, 120-124.

Barr, M. L. and Bertram, E. G. (1949). A morphological distiction between neurons of the male and female and the behaviour of the nucleolar satellite during accelerated nucleoprotein synthesis. *Nature* **163**, 676-677.

Boggs, B. A., Cheung, P., Heard, E., Spector, D. L., Chinault, A. C. and Allis, C. D. (2002). Differentially methylated forms of histone H3 show unique association patterns with inactive human X chromosomes *Nat. Genet.* **1**, 73-76.

Bongiorni, S., Cintio, O. and Prantera, G. (1999). The relationship between DNA methylation and chromosome imprinting in the coccid *Planococcus citri*. *Genetics* **151**, 1471-1478.

Bongiorni, S., Mazzuoli, M., Masci, S. and Prantera, G. (2001). Facultative heterochromatization in parahaploid male mealybugs: involvement of heterochromatin-associated protein. *Development* **128**, 3809-3817.

Bouniol-Baly, C., Nguyen, E., Besombes, D. and Debey, P. (1997). Dynamic organization of DNA replication in one-cell mouse embryos: relationship to transcriptional activation *Exp. Cell Res.* **236**, 201-211.

Brown, S. W. (1966). Heterochromatin. *Science* **151**, 417-425.

Brown, S. W. and Nur, U. (1964). Heterochromatic chromosomes in *Coccids*. *Science* **145**, 130-136.

Chadwick, B. P. and Willard, H. F. (2003). Chromatin of the Barr body: histone and non-histone proteins associated with or excluded from the inactive X chromosome. *Hum. Mol. Genet.* **12**, 2167-2178.

Cowell, I. G., Aucott, R., Mahadevaiah, S. K., Burgoyne, P. S., Huskisson, N., Bongiorni, S., Prantera, G., Fanti, L., Pimpinelli, S., Wu, R., et al. (2002). Heterochromatin, HP1 and methylation at lysine 9 of histone H3 in animals. *Chromosoma* **111**, 22-36.

De Silva, B. S., Egodage, K. L. and Wilson, G. S. (1999). Purified protein derivative (PPD) as an immunogen carrier elicits high antigen specificity to haptens. *Bioconjug. Chem.* **10**, 496-501.

Epstein, H., James, T. C. and Singh, P. B. (1992). Cloning and expression of Drosophila HP1 homologs from a mealybug, *Planococcus citri*. *J. Cell Sci.* **101**, 463-474.

Fang, J., Feng, Q., Ketel, C. S., Wang, H., Cao, R., Xia, L., Erdjument-Bromage, H., Tempst, P., Simon, J. A. and Zhang, Y. (2002). Purification and functional characterization of SET8, a nucleosomal histone H4-lysine 20-specific methyltransferase. *Curr. Biol.* **12**, 1086-1099.

Gilbert, D. M. and Cohen, S. N. (1987). Bovine papilloma virus plasmids replicate randomly in mouse fibroblasts throughout S phase of the cell cycle. *Cell* **50**, 59-68.

Heitz, E. (1928). Das Heterochromatin der Moose I. *Jahrb. Wissensch. Bot.* **69**, 762-818.

Jacobs, S. A., Taverna, S. D., Zhang, Y., Briggs, S. D., Li, J., Eissenberg, J. C., Allis, C. D. and Khorasanizadeh, S. (2001). Specificity of the HP1 chromo domain for the methylated N-terminus of histone H3. *EMBO J.* **20**, 5232-5241.

James, T. C., Eissenberg, J. C., Craig, C., Dietrich, V., Hobson, A. and Elgin, S. C. (1989). Distribution patterns of HP1, a heterochromatin-

associated nonhistone chromosomal protein of *Drosophila*. *Eur. J. Cell Biol.* **50**, 70-80.

Jeppesen, P. and Turner, B. M. (1993). The inactive X chromosome in female mammals is distinguished by a lack of histone H4 acetylation, a cytogenetic marker for gene expression. *Cell* **74**, 281-289.

Jeppesen, P., Mitchell, A., Turner, B. and Perry, P. (1992). Antibodies to defined histone epitopes reveal variations in chromatin conformation and underacetylation of centric heterochromatin in human metaphase chromosomes. *Chromosoma* **101**, 322-332.

John, B. and Miklos, G. L. (1979). Functional aspects of satellite DNA and heterochromatin. *Int. Rev. Cytol.* **58**, 1-114.

Kafri. T., Gao, X. and Razin, A. (1993). Mechanistic aspects of genome-wide demethylation in the preimplantation mouse embryo. *Proc. Natl. Acad. Sci. USA* **90**, 10558-10562.

Lachner, M., O'Carroll, D., Rea, S., Mechtler, K. and Jenuwein, T. (2001). Methylation of histone H3 lysine 9 creates a binding site for HP1 proteins. *Nature* **410**, 116-120.

Lima-de-faria, A. and Jaworska, H. (1968). Late DNA synthesis in heterochromatin. *Nature* **217**, 138-142.

Lyon, M. F. (1999). Imprinting and X-chromosome inactivation. *Results Probl. Cell Differ.* **25**, 73-90.

Maison, C., Horstmann, H. and Georgatos, S. D. (1993). Regulated docking of nuclear membrane vesicles to vimentin filaments during mitosis. *J. Cell Biol.* **123**, 1491-1505.

Maison, C., Pyrpasopoulou, A. and Georgatos, S. D. (1995). Vimentin-associated mitotic vesicles interact with chromosomes in a lamin B- and phosphorylation-dependent manner. *EMBO J.* **14**, 3311-3324.

Mayer, W., Niveleau, A., Walter, J., Fundele, R. and Haaf, T. (2000). Demethylation of the zygotic paternal genome. *Nature* **403**, 501-502.

McClintock, B. (1934). The relation of a particular chromosomal element to the development of the nucleoli in *Zea mays*. *Z. Zellforsch. Mikrosk. Anat.* **21**, 294-328.

Miller, O. J., Schnedl, W., Allen, J. and Erlanger, B. F. (1974). 5-Methylcytosine localised in mammalian constitutive heterochromatin. *Nature* **251**, 636-637.

Monk, M., Boubelik, M. and Lehnert, S. (1987). Temporal and regional changes in DNA methylation in the embryonic, extraembryonic and germ cell lineages during mouse embryo development. *Development* **99**, 371-382.

Morrison, H. and Jeppesen, P. (2002). Allele-specific underacetylation of histone H4 downstream from promoters is associated with X-inactivation in human cells. *Chromosome Res.* **10**, 579-595.

Morishima, A., Grumbach, M. and Taylor, J. H. (1962). Asynchronous duplication of human chromosomes and the origin of sex chromatin. *Proc. Natl. Acad. Sci. USA* **48**, 756-763.

Nishioka, K., Rice, J. C., Sarma, K., Erdjument-Bromage, H., Werner, J., Wang, Y., Chuikov, S., Valenzuela, P., Tempst, P., Steward, R., et al. (2002). PR-Set7 is a nucleosome-specific methyltransferase that modifies lysine 20 of histone H4 and is associated with silent chromatin. *Mol. Cell* **9**, 1201-1213.

Oswald, J., Engemann, S., Lane, N., Mayer, W., Olek, A., Fundele, R., Dean, W., Reik, W. and Walter, J. (2000). Active demethylation of the paternal genome in the mouse zygote. *Curr. Biol.* **10**, 475-478.

Pardue, M. L. and Gall, J. G. (1970). Chromosomal localisation of mouse satellite DNA. *Science* **168**, 1356-1358.

Peters, A. H., Plug, A. W. and de Boer, P. (1997). Meiosis in carriers of heteromorphic bivalents: sex differences and implications for male fertility. *Chromosome Res.* **5**, 313-324.

Peters, A. H., O'Carroll, D., Scherthan, H., Mechtler, K., Sauer, S., Schofer, C., Weipoltshammer, K., Pagani, M., Lachner, M., Kohlmaier, A., et al. (2001). Loss of the Suv39h histone methyltransferases impairs mammalian heterochromatin and genome stability. *Cell* **107**, 323-337.

Peters, A. H., Mermoud, J. E., O'Carroll, D., Pagani, M., Schweizer, D., Brockdorff, N. and Jenuwein, T. (2002). Histone H3 lysine 9 methylation is an epigenetic imprint of facultative heterochromatin. *Nat. Genet.* **30**, 77-80.

Pimpinelli, S., Bonnaccorsi, J., Gatti, M. and Sandler, L. (1986). The peculiar genetic organisation of *Drosophila* heterochromatin. *Trends Genet.* **2**, 17-20.

Plath, K., Fang, J., Mlynarczyk-Evans, S. K., Cao, R., Worringer, K. A., Wang, H., de la Cruz, C. C., Otte, A. P., Panning, B. and Zhang, Y. (2003). Role of histone H3 lysine 27 methylation in X inactivation. *Science* **300**, 131-135.

Pratt, H. P. (2001). Isolation and culture of pre-implantation embryos. In *Mammalian Development – a practical approach* (ed. M. Monk), pp. 15-43. Oxford: IRL Press.

Rea, S., Eisenhaber, F., O'Carroll, D., Strahl, B. D., Sun, Z. W., Schmid, M., Opravil, S., Mechtler, K., Ponting, C. P., Allis, C. D., et al. (2000). Regulation of chromatin structure by site-specific histone H3 methyltransferases. *Nature* **406**, 593-599.

Rice, J. C., Nishioka, K., Sarma, K., Steward, R., Reinberg, D. and Allis, C. D. (2002). Mitotic-specific methylation of histone H4 Lys 20 follows increased PR-Set 7 expression and its localization to mitotic chromosomes. *Genes Dev.* **16**, 2225-2230.

Santos-Rosa, H., Schneider, R., Bannister, A. J., Sherriff, J., Bernstein, B. E., Emre, N. C., Schreiber, S. L., Mellor, J. and Kouzarides, T. (2002). Active genes are tri-methylated at K4 of histone H3. *Nature* **419**, 407-411.

Sarg, B., Koutzamani, E., Helliger, W., Rundquist, I. and Lindner, H. H. (2002). Postsynthetic trimethylation of histone H4 at lysine 20 in mammalian tissues is associated with aging. *J. Biol. Chem.* **277**, 39195-39201.

Singh, P. B. and Huskisson, N. S. (1998). Chromatin complexes as aperiodic microcrystalline arrays that regulate genome organisation and expression. *Dev. Genet.* **22**, 85-99.

Solari, A. J. (1974). The behavior of the XY pair in mammals. *Int. Rev. Cytol.* **38**, 273-317.

Starbuck, W. C., Mauritzen, C. M., Taylor, C. W., Saroja, I. S. and Busch, H. (1968). A large scale procedure for isolation of the glycine-rich, arginine-rich histone and the arginine-rich, lysine-rich histone in a highly purified form. *J. Biol. Chem.* **243**, 2038-2047.

Tamaru, H., Zhang, X., McMillen, D., Singh, P. B., Nakayama, J., Grewal, S. I., Allis, C. D., Cheng, X. and Selker, E. U. (2003). Trimethylated lysine 9 of histone H3 is a mark for DNA methylation in *Neurospora crassa*. *Nat. Genet.* **34**, 75-79.

Turner, J. M., Burgoyne, P. S. and Singh, P. B. (2001). M31 and macroH2A1.2 colocalise at the pseudoautosomal region during mouse meiosis. *J. Cell Sci.* **114**, 3367-3375.

Von Glasenapp, E. and Benavente, R. (2000). Fate of meiotic lamin C2 in rat spermatocytes cultured in the presence of okadaic acid. *Chromosoma* **109**, 117-122.

Wu, J. R., Yu, G. and Gilbert, D. M. (1997). Origin-specific initiation of mammalian nuclear DNA replication in a *Xenopus* cell-free system. *Methods* **13**, 313-324.